Breast Cancer Res Treat (2017) 161:17–28
DOI 10.1007/s10549-016-4036-0

PRECLINICAL STUDY

Characterizing the immune microenvironment in high-risk ductal carcinoma in situ of the breast

Michael J. Campbell[1] · Frederick Baehner[2] · Tess O'Meara[3] · Ekene Ojukwu[3] · Booyeon Han[3] · Rita Mukhtar[1] · Vickram Tandon[3] · Max Endicott[3] · Zelos Zhu[3] · Jasmine Wong[1] · Gregor Krings[2] · Alfred Au[2] · Joe W. Gray[4] · Laura Esserman[1,3]

Received: 19 October 2016 / Accepted: 21 October 2016 / Published online: 26 October 2016

Abstract
Purpose The recent increase in the incidence of ductal carcinoma in situ (DCIS) has sparked debate over the classification and treatment of this disease. Although DCIS is considered a precursor lesion to invasive breast cancer, some DCIS may have more or less risk than is realized. In this study, we characterized the immune microenvironment in DCIS to determine if immune infiltrates are predictive of recurrence.
Methods Fifty-two cases of high-grade DCIS (HG-DCIS), enriched for large lesions and a history of recurrence, were age matched with 65 cases of non-high-grade DCIS (nHG-DCIS). Immune infiltrates were characterized by single- or dual-color staining of FFPE sections for the following antigens: CD4, CD8, CD20, FoxP3, CD68, CD115, Mac387, MRC1, HLA-DR, and PCNA. Nuance multispectral imaging software was used for image acquisition. Protocols for automated image analysis were developed using CellProfiler. Immune cell populations associated with risk of recurrence were identified using classification and regression tree analysis.
Results HG-DCIS had significantly higher percentages of FoxP3$^+$ cells, CD68$^+$ and CD68$^+$PCNA$^+$ macrophages, HLA-DR$^+$ cells, CD4$^+$ T cells, CD20$^+$ B cells, and total tumor infiltrating lymphocytes compared to nHG-DCIS. A classification tree, generated from 16 immune cell populations and 8 clinical parameters, identified three immune cell populations associated with risk of recurrence: CD8$^+$HLADR$^+$ T cells, CD8$^+$HLADR$^-$ T cells, and CD115$^+$ cells.
Conclusion These findings suggest that the tumor immune microenvironment is an important factor in identifying DCIS cases with the highest risk for recurrence and that manipulating the immune microenvironment may be an efficacious strategy to alter or prevent disease progression.

Keywords DCIS · Breast · Immune microenvironment

Introduction

Ductal carcinoma in situ (DCIS) is a non-obligate precursor of invasive breast carcinoma that is characterized by the confinement of proliferating ductal cells, with malignant features, to within the basement membrane of mammary ducts [1]. Pure DCIS, as well as DCIS with micro-invasion (DCIS lesions with an invasive component of 0.1 cm or less), is typically thought to have a very low risk of recurrence and death [2–4]. The risk for development of a potentially lethal invasive cancer, however, is thought to be sufficient to warrant an aggressive surgical approach. As such, treatment includes surgical excision and generally radiation therapy or mastectomy. For hormone receptor-positive DCIS, risk reducing endocrine therapy is offered unless bilateral mastectomy is performed, while chemotherapy is not offered.

While aggressive disease comprises only a small percentage of DCIS cases, less aggressive DCIS tumors

✉ Michael J. Campbell
michael.campbell@ucsf.edu

[1] Department of Surgery, University of California, 2340 Sutter St, N321, San Francisco, CA 94115, USA

[2] Department of Pathology, University of California, San Francisco, CA, USA

[3] Mt Zion Carol Franc Buck Breast Care Center, University of California, San Francisco, CA, USA

[4] Oregon Health and Science University, Portland, OR, USA

are often treated with the same therapies, resulting in the overtreatment of many DCIS patients [5]. At the other extreme, however, is the infrequent but equally concerning potential for undertreatment. Recently, an evaluation of 100,000 cases of DCIS revealed that there is a small group of women diagnosed with DCIS that develop metastatic disease without first developing an invasive cancer recurrence who are at risk of dying from their disease [6]. Importantly, current treatments do not prevent death. We therefore need the ability to characterize the highest risk DCIS lesions and their underlying biology so that we can develop and test more appropriate treatments.

DCIS lesions with a greater chance of disease recurrence or progression are categorized by a number of biological factors including high histologic nuclear grade and comedonecrosis [7–12], tumor size and pathological density [13, 14], and palpability [15]. The University of Southern California/Van Nuys Prognostic Index (USC/VNPI) was devised by combining four statistically significant independent prognostic factors for local recurrence: tumor size, margin width, age, and pathological classification (determined by nuclear grade and the presence or absence of comedo-type necrosis) [16, 17]. While these associations have proven beneficial in categorizing DCIS lesions, and directing local therapy, these markers are not sufficient to identify the group at risk of death from their DCIS nor to predict what therapy might prevent that event.

The tumor immune microenvironment clearly plays a role in the progression of invasive breast cancer. Tumor-associated macrophages (TAMs), regulatory T cells (Treg), type 2 helper T cells (Th2), and myeloid-derived suppressor cells (MDSC) are associated with a suppressive immune microenvironment and poor outcomes, while other cells such as cytotoxic T cells (Tc), type 1 helper T cells (Th1), and natural killer cells (NK) are associated with an anti-tumor immune microenvironment and good outcomes [18–29]. In contrast, the immune landscape of DCIS has not been well characterized. Increased inflammation in DCIS is associated with high nuclear grade, HER2 positivity, and extent of lesions [30, 31]. FoxP3+ Tregs have been identified in DCIS lesions, although they were not associated with grade [32]. Esserman and coworkers found that $CD68^{+}$ macrophages were associated with large, pathologically dense, high-grade DCIS lesions with comedonecrosis [13]. High-grade DCIS lesions are also associated with a macrophage response signature [33].

In this study, we characterized and compared the immune microenvironments in high-grade DCIS (HG-DCIS) and non-high-grade DCIS (nHG-DCIS) and sought to determine if immune infiltrates are predictive of recurrence and metastasis.

Materials and methods

Sample collection

One hundred and seventeen archived paraffin blocks (collected between 1994 and 2014) were retrieved from the UCSF breast oncology program tumor bank with IRB approval (see CONSORT Diagram, Fig. 1). Fifty-two cases of high-grade DCIS (HG-DCIS), enriched for large lesions and a history of recurrence, were age- and size-matched with 65 cases of non-high-grade DCIS (nHG-DCIS). This study was conducted to better understand the biology/immunology of high-grade, high-risk DCIS. Since we selected for a cohort of high-grade DCIS and an age- and size-matched cohort of non-high-grade DCIS, the overall study population is biased towards more high-grade cases and larger lesions compared to a non-selected population.

Pathologic characteristics including tumor stage, grade, size, composition, and hormone receptor status [ER and PR assessed by standard immunohistochemistry (IHC)] were obtained from pathology reports. HER2 and Ki67 were determined by standard IHC on freshly cut sections as a

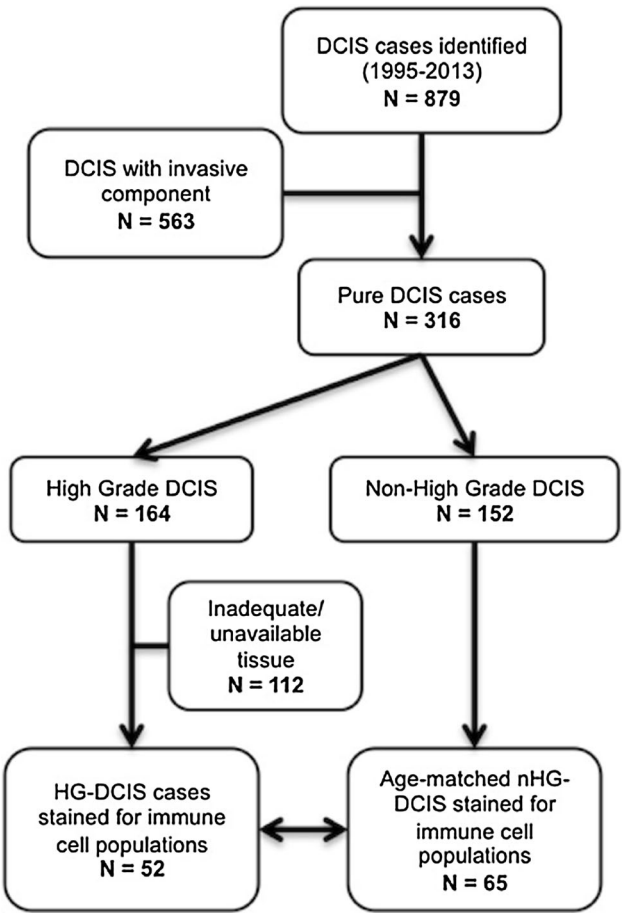

Fig. 1 CONSORT diagram of DCIS cohorts selected for immune marker staining

part of this study. HER2 status was not confirmed by FISH for this study. Patient characteristics and clinical parameters including age, palpability, surgery type, and recurrence were obtained by medical record review. Van Nuys Prognostic Index scores (VNPI; 12-point scale) were calculated based on margins, age, and grade as previously reported [16, 17]. Breast density was determined radiographically and classified into the standard four BI-RADS groups by a radiologist. DCIS density was determined from H&E-stained slides as previously described [13].

Manual TIL counts

Tumor infiltrating lymphocytes (TIL) were visually identified by a pathologist on 5-μm H&E-stained sections, based on morphology and size. TILs identified within the DCIS lesions (itTILs) were manually counted in 10 high power fields (HPF; 400X) and the average number of TILs per HPF was calculated for each case. Stromal TILs (stTILs) were visually estimated as a percentage of total stroma per section and assigned a score of 1–4 (1: ≤1%; 2: >1 and ≤5%; 3: >5 and ≤10%; 4: >10%).

Immunohistochemistry

Antibodies and their respective dilutions used in this study are listed in Table 1. Formalin-fixed, paraffin-embedded tumor blocks were cut into 5-μm sections, deparaffinized in xylene and rehydrated using graded ethanol. Antigen retrieval was performed with pressure cooking in 10 mM citrate buffer for 10 min. This was followed by application of an endogenous enzyme block and subsequent protein block to prevent non-specific antibody binding. Single-marker stains were performed with a standard streptavidin–biotin peroxidase method using the Vectastain ABC-HRP labeling kit (Vector Labs) and DAB as a substrate. Single color stains were performed for the following antigens: CD115 and FoxP3. Two-color immunohistochemistry was performed using the EnVision G/2 Doublestain System (DAB+/Permanent Red; Dako). Dual-marker staining was performed for the following antigen pairs: CD68/PCNA, CD68/MAC387, CD68/MRC1, CD8/HLA-DR, and CD4/CD20. Slides were counterstained with hematoxylin to aid identification of nuclei in subsequent image analyses.

Multispectral imaging

For each case, 3 hot spots based on CD68/Mac387 staining were manually identified by a pathologist and marked on 10 consecutive sections. Images were captured from these marked regions for each single- or dual-stained slide. Using CD8/HLADR staining as the criterion to identify hotspots resulted in similar results (data not shown). Two colors (DAB and hematoxylin) on single-stained slides or three colors (DAB, Permanent Red, and hematoxylin) on dual-stained slides were imaged using the Nuance FX imaging system (CRI). Pure chromogen control slides (DAB, Permanent Red, or hematoxylin) were prepared as described above using a single antibody (or no antibody for the hematoxylin control). These control, single color slides were used to generate spectral libraries of each chromogen used in the study. Settings on the microscope and camera were kept consistent for all image cubes taken. Images (at 200× magnification) were obtained at 20-nm intervals across a range of 420–720 nm to create image cubes which were then spectrally unmixed into two or three individual monochrome images (one for each color) for subsequent image analyses.

Automated image analysis

Pipelines were developed in CellProfiler software (Broad Institute [34, 35]) to analyze the unmixed monochrome images obtained from the Nuance system. Cell nuclei were

Table 1 Panel of primary antibodies used in this study

Antigen	Antibody clone	Dilution	Source
CD4 (T cell marker)	4B12	1:80	Labvision (#MS-1528S)
CD8 (T cell marker)	C8/144b	1:400	Dako (#M7103)
CD20 (B cell marker)	L26	1:400	Dako (#M0755)
CD68 (macrophage marker)	PGM1	1:400	Dako (#M0876)
HLA-DR, DP, DQ (Major histocompatibility complex, class II)	CR3/43	1:320	Abcam (#ab7856)
S100A8/A9 (calprotectin)	MAC387	1:6400	Dako (#M0747)
MRC1 (mannose receptor, C type 1)	M02	1:100	Abgent (#AT2899a)
PCNA (proliferating cell nuclear antigen)	PC10	1:2000	Dako (#M0879)
CSF-1R/CD115/c-fms (colony stimulating factor 1 receptor)	Rabbit polyclonal	1:100	Santa Cruz (#sc-692)
FoxP3 (forkhead box P3, scurfin)	236A/E7	1:200	Abcam (#ab20034)

first identified using the unmixed hematoxylin image and an Otsu Global thresholding method. Images were then segmented into cells using an annulus approach. Since there was not always a secondary stain to help identify cell edges, the nuclei were simply expanded in order to estimate the cell's location. Staining intensities for DAB and/or Permanent Red were then calculated for each cell. Single and double positive cells were classified based on preset thresholds determined from control (no primary antibody) stained slides and were scored as a percentage of total cells averaged over three 200X fields. Counts of intratumoral (i.t.) $CD8^+$ cells, i.t. HLA-DR^+ cells, and measurement of CD115 intensity staining on DCIS epithelial cells were obtained from manually created masks within a CellProfiler pipeline.

Statistical analysis

The associations between clinicopathologic parameters in the HG-DCIS and nHG-DCIS cohorts were tested with Fisher's exact test for 2×2 or 2×3 comparisons. Spearman's correlation test was used to assess the correlations between manual and automated cell counts, as well as the relationship between immune cell populations and clinicopathologic characteristics. Mean differences of immune cell populations in the HG-DCIS and nHG-DCIS cohorts were determined with the Student's t test. Correlation network analyses and maps were visualized in R with the igraph package. Communities of cell types were determined using the walktrap function, which finds densely connected subgraphs (communities) in a graph via random walks. Classification trees were produced using a Recursive Partitioning and Regression Trees (RPART) analysis in R with tenfold cross validation (rpart and rpart.plot libraries). Trees were generated from immune population data combined with clinical parameters. Kaplan–Meier recurrence-free survival curves were calculated and plotted in R using the "survival" library and the "survfit" function. Differences between curves were compared using the χ^2 statistic ("survdiff" function).

Results

Clinical characteristics of patient cohorts

The clinicopathologic characteristics of DCIS cases in this study are presented in Tables 2 and 3. The median age for the entire cohort was 47 years (range 26–79 years). Both the HG-DCIS and the nHG-DCIS cohorts showed similar age distributions. The HG-DCIS lesions demonstrated more comedonecrosis and were skewed towards hormone receptor negativity, HER2 positivity, higher proliferation (Ki67), and higher VNPI scores compared to the nHG-DCIS lesions. The median follow-up time for the entire cohort was 7.1 years (range 0.1–16.2 years). There were 18 relapses in this DCIS series, which included six local recurrences of DCIS, eight local/contralateral invasive tumors, and four metastatic events.

The immune landscape of DCIS

DCIS samples were stained for immune markers and analyzed using an integrated image analysis approach. The Nuance imaging system unmixes spectra from the various chromogens used and the resulting unmixed images were then analyzed using custom pipelines developed in CellProfiler software. Figure 2 shows examples of cases with low and high numbers of various immune cell infiltrates.

To determine the concordance between automated scoring and manual scoring, subsets of cases were visually scored by a pathologist who was blinded to the automated image analysis results. Cases were selected that spanned a range from low to high counts for the given marker as measured by the automated counting algorithms. Visual scores/counts were highly correlated with the automated counts for single- and two-color stained populations (Fig. 3). Since TILs are composed mainly of T and B lymphocytes, summing the automated counts for $CD4^+$ and $CD8^+$ cells (T lymphocytes) with $CD20^+$ cells (B lymphocytes) yielded an automated TIL count. There was good concordance between this automated TIL count and the manual score for TILs (Fig. 3).

Correlation network maps were constructed to investigate the relationships between immune cell populations in HG-DCIS versus nHG-DCIS (Fig. 4). In the nHG-DCIS cohort, the immune cell populations clustered into two groups: one containing the macrophage populations ($CD68^+$, $CD68^+MRC1^+$, $CD68^+Mac387^+$, with the exception of the $CD68^+PCNA^+$ population) along with the $CD115^+$ population and a second group containing the lymphocyte populations. In the HG-DCIS cohort, the lymphocyte populations were split into two clusters: one containing the $CD4^+$, $CD20^+$, and TILs populations and the other containing the $CD8^+$ and the HLA-DR^+ populations, as well as the $FoxP3^+$ cells. The macrophages clustered together, as in the nHG-DCIS cohort, but the $CD115^+$ population in the HG-DCIS cases clustered with the HLA-DR^+, $CD8^+$ and $FoxP3^+$ populations, not with the macrophage cluster as in the nHG-DCIS cohort.

Immune cell populations in HG-DCIS vs nHG-DCIS and correlations with clinicopathologic parameters

The percentages of each immune cell population in nHG-DCIS (gray boxes) and HG-DCIS (white boxes) are shown

Table 2 Characteristics of study cohorts

	All DCIS ($n = 117$)	nHG-DCIS ($n = 65$)	HG-DCIS ($n = 52$)	nHG-DCIS versus HG-DCIS
	No. (%)	No. (%)	No. (%)	p value[a]
Age				
≤39	17 (15)	11 (17)	6 (12)	N.S.[b]
40–60	79 (68)	41 (63)	38 (73)	
≥60	21 (18)	13 (20)	8 (15)	
Tumor size				
≤15 mm	40 (34)	26 (40)	14 (27)	N.S.
16–40 mm	36 (31)	20 (31)	16 (31)	
≥41 mm	41 (35)	19 (29)	22 (42)	
Margins				
≥10 mm	34 (29)	21 (32)	13 (25)	N.S.
1–9 mm	55 (47)	31 (48)	24 (46)	
<1 mm	28 (24)	13 (20)	15 (29)	
Comedonecrosis				
No	36 (31)	28 (43)	8 (15)	0.001
Yes	81 (69)	37 (57)	44 (85)	
HR status				
Neg	35 (30)	12 (18)	21 (40)	0.013
Pos	82 (70)	53 (82)	31 (60)	
HER2 status				
Neg/1+	32 (27)	21 (33)	11 (22)	0.031
2+	15 (13)	12 (19)	3 (6)	
3+	66 (56)	31 (48)	35 (71)	
Not available	4 (3)	1 (2)	3 (6)	
Ki67				
Low (≤15%)	47 (40)	34 (52)	13 (25)	0.025
Intermediate	32 (27)	18 (28)	14 (27)	
High (>30%)	19 (16)	7 (11)	12 (23)	
Not available	19 (16)	6 (9)	13 (25)	
Breast density				
1	8 (7)	6 (9)	2 (4)	N.S.
2	27 (23)	16 (25)	11 (21)	
3	50 (43)	26 (40)	24 (46)	
4	17 (15)	12 (18)	5 (10)	
Not available	15 (13)	5 (8)	10 (19)	
DCIS density				
1	23 (20)	16 (25)	7 (13)	N.S.
2	26 (22)	15 (23)	11 (21)	
3	45 (38)	23 (35)	22 (42)	
Not available	23 (20)	11 (17)	12 (23)	

Table 2 continued

	All DCIS ($n = 117$) No. (%)	nHG-DCIS ($n = 65$) No. (%)	HG-DCIS ($n = 52$) No. (%)	nHG-DCIS versus HG-DCIS p value[a]
Van Nuys Prognostic Index				
4–6	16 (14)	14 (22)	2 (4)	0.003
7–9	64 (55)	37 (57)	27 (52)	
10–12	37 (32)	14 (22)	23 (44)	

[a] By Fisher exact test

[b] Not significant

Table 3 Recurrence events, surgery, and adjuvant therapies

	All DCIS ($n = 117$) No. (%)	nHG-DCIS ($n = 65$) No. (%)	HG-DCIS ($n = 52$) No. (%)
Recurrence events			
No events	99 (85)	57 (88)	42 (81)
Any event	18 (15)	8 (12)	10 (19)
DCIS recurrence	6 (33)	4 (50)	2 (20)
Invasive events	12 (67)	4 (50)	8 (80)
Recurrence by surgery type			
Lumpectomy			
No events	56 (84)	36 (86)	20 (80)
DCIS recurrence	6 (9)	4 (10)	2 (8)
Local/contralateral invasive events	5 (7)	2 (5)	3 (12)
Metastatic events	0 (0)	0 (0)	0 (0)
Mastectomy			
No events	43 (86)	21 (91)	22 (81)
DCIS recurrence	0 (0)	0 (0)	0 (0)
Local/contralateral invasive events	3 (6)	1 (4)	2 (7)
Metastatic events	4 (8)	1 (4)	3 (11)
Adjuvant therapy			
None	57 (49)	35 (54)	22 (42)
Tamoxifen only	11 (9)	6 (9)	5 (10)
XRT only	29 (25)	18 (28)	11 (21)
XRT + tamoxifen	10 (9)	2 (3)	8 (15)
Other	3 (3)	2 (3)	1 (2)
Not available	7 (6)	2 (3)	5 (10)

in Fig. 5a. HG-DCIS had significantly higher percentages of FoxP3$^+$ cells (Treg), CD68$^+$ macrophages, CD68$^+$-PCNA$^+$ macrophages, HLA-DR$^+$ cells, CD4$^+$ T cells, CD20$^+$ B cells, and TILs (sum of CD4$^+$, CD8$^+$, and CD20$^+$ cells) compared to nHG-DCIS.

Examining correlations between immune cell populations and clinical characteristics of all 117 DCIS cases, we found that overall, immune infiltrates tended to be correlated with high-risk features (Fig. 5b). CD68$^+$ macrophages were correlated with high VNPI, palpability, high-grade, comedonecrosis, Ki67 positivity, and HR negativity. Similar results were seen for the Mac387$^+$ cells and the dual positive CD68$^+$Mac387$^+$ cells. Interestingly, the CD68$^+$MRC1$^+$ cells (M2-type macrophages) were not significantly correlated with any clinical parameters. CD115, the CSF-1 receptor, was expressed on both

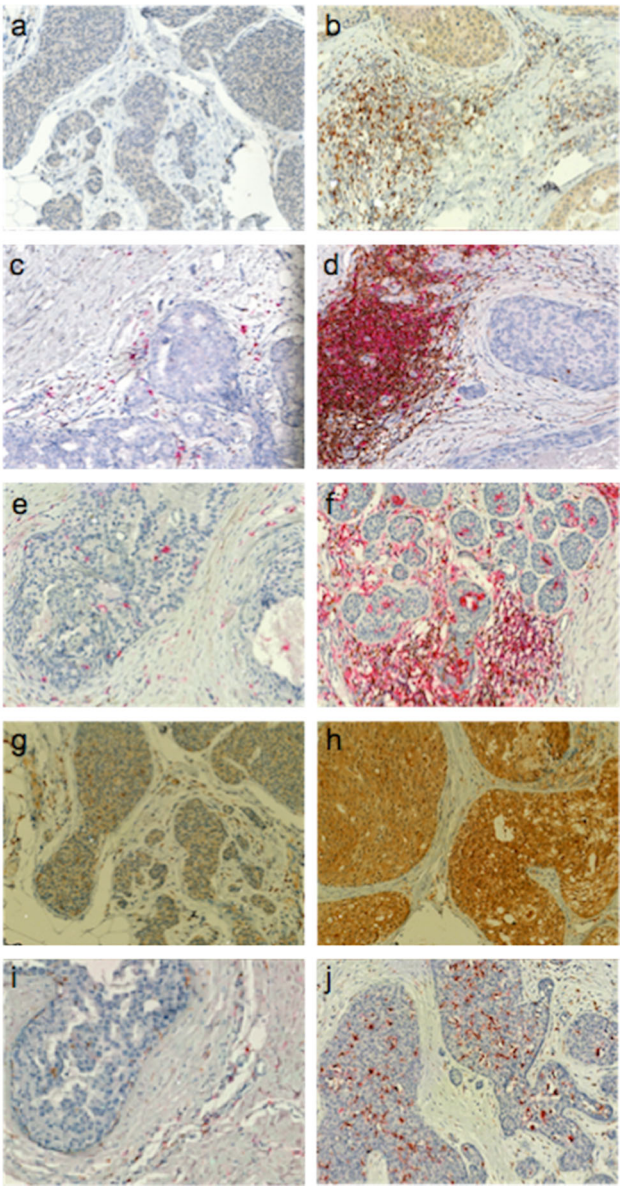

Fig. 2 Immunohistochemical detection of immune cell populations in DCIS. **a** and **b** FoxP3 (*brown*); **c** and **d** CD4 (*brown*) & CD20 (*red*); **e** and **f** CD8 (*brown*) & HLA-DR (*red*); **g** and **h** CD115 (*brown*); **i** and **j** CD68 (*brown*) & MRC1 (*red*)

macrophages and the DCIS epithelial cells. $CD115^+$ macrophages correlated with high Ki67 and HER2 positivity, while CD115 expression on the DCIS lesions correlated with high Ki67, HER2 positivity, high-grade, and HR negativity.

With respect to lymphocyte infiltrates, $CD4^+$ T cells, $CD20^+$ B cells, and total TILs ($CD4^+$, $CD8^+$, and $CD20^+$ cells) were associated with high-risk features (VNPI, large tumor size, high-grade, comedonecrosis, high Ki67, HER2 positivity, and HR negativity). $CD8^+$ cells were correlated with high-grade, HER2 positivity, and HR negativity, but not with other high-risk features such as VNPI, size, or comedonecrosis. Interestingly, the intratumoral (cells within the DCIS involved ducts) $CD8^+$ or $HLADR^+$ cells tended to be associated with low-risk features (not palpable, low grade, no comedonecrosis) and a low DCIS density score.

Immune cell populations as markers of clinical outcome

Comparing the mean percentages of immune cell populations in cases with a recurrence versus those without, we found no cell types that, by themselves, were associated with outcomes. We then constructed a prognostic model using the RPART function in R. A classification tree was generated using as input 16 immune cell populations along with 8 clinical parameters (grade, VNPI, tumor size, palpable, comedonecrosis, HR status, HER2 status, and DCIS density). Of the 24 input parameters, the best RPART model was built using only 3 immune cell populations: $CD8^+HLADR^+$ cells, $CD8^+HLADR^-$ cells and $CD115^+$ cells (Fig. 6a). This model had an accuracy of 87% (sensitivity = 76%; specificity = 89%). Importantly, all four cases with metastatic recurrences were correctly predicted.

Recurrence-free survival curves according to this model are shown in Fig. 6b. The highest risk of recurrence was in cases with low numbers of activated $CD8^+HLADR^+$ cells (node 4). Cases not only with high $CD8^+HLADR^+$ cells, but also high numbers of non-activated $CD8^+HLADR^-$ cells and high numbers of $CD115^+$ cells were also at a high risk for recurrence (node 3). In contrast, cases with high $CD8^+HLADR^+$ cells and low $CD8^+HLADR^-$ cells (node 1) or high $CD8^+HLADR^+$ cells, high $CD8^+HLADR^-$ cells, and low $CD115^+$ cells (node 2) were at a low risk for recurrence. There was no significant difference in recurrence-free survival between the nHG-DCIS and the HG-DCIS cohorts (Fig. 6c), nor when stratified by VNPI (Fig. 6d).

Discussion

Several studies have shown a clear association between lymphocyte and/or macrophage infiltration and prognosis in human invasive breast cancer; [18–29] however, the role of these cells in the prognosis of DCIS is unclear. In this study, we characterized the immune landscape of DCIS and asked whether certain populations of immune cells were associated with high-grade DCIS and if these might provide markers and etiology for risk of recurrence. We would like to emphasize that, due to the lack of a validation cohort, this should be considered an exploratory/descriptive study.

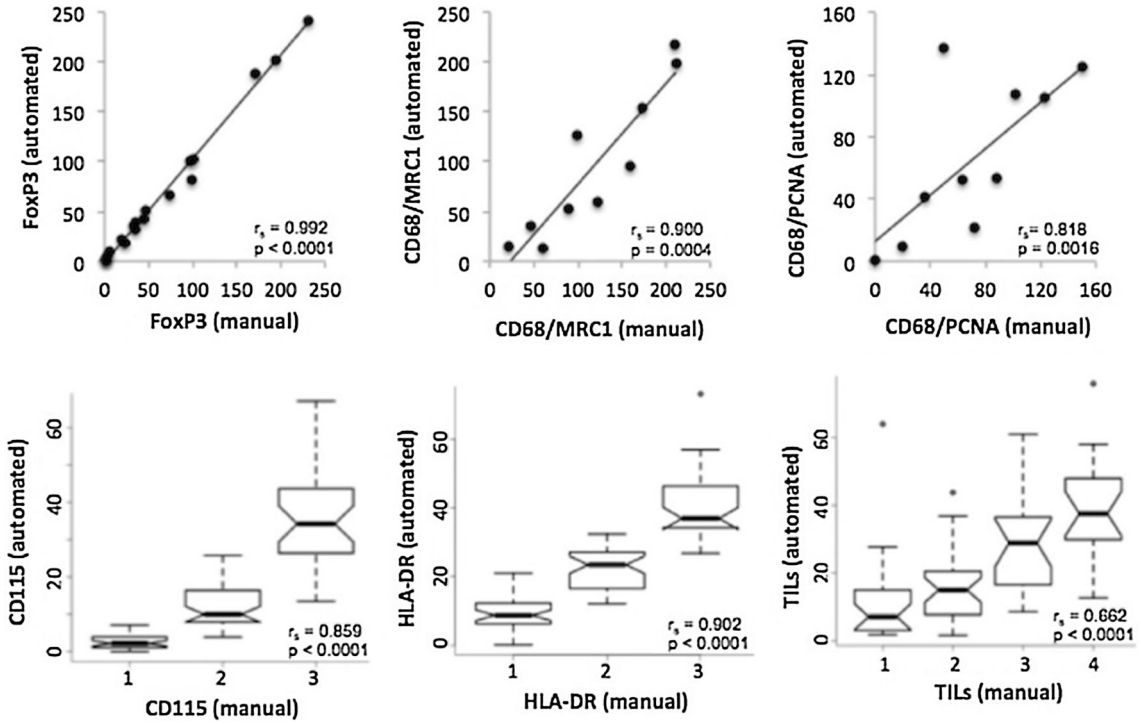

Fig. 3 Comparison between visual (manual) counting assessment and automated counting assessment of immune markers in DCIS. Scatter plots are shown for comparisons of manual with automated cell counts (cells per 200X field). Box plots are shown for comparisons of manual scoring (low to high) with automated cell counts given as a percentage of total cells. (r_s and p values, Spearman correlation). Similar results were seen for the other staining panels (data not shown)

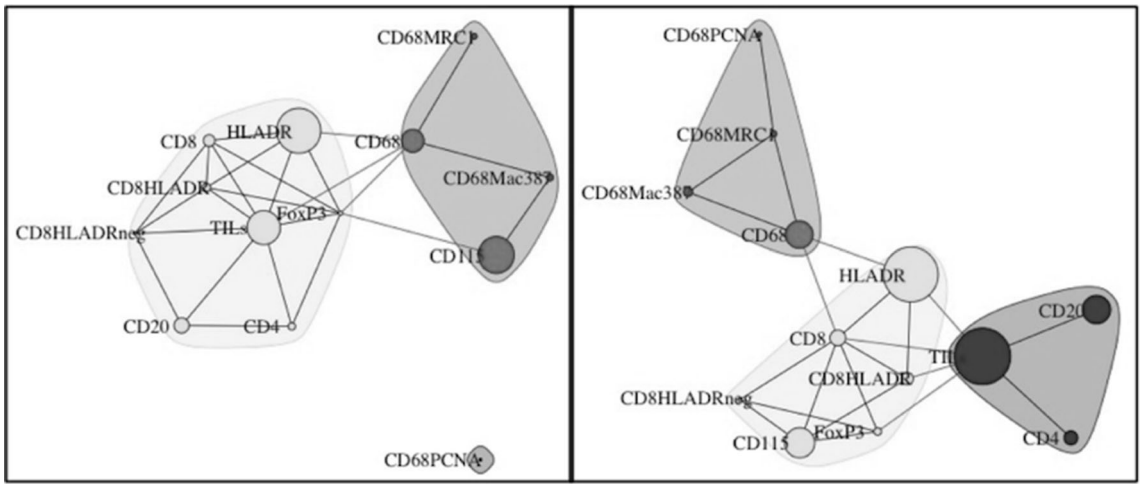

Fig. 4 The immune landscape in DCIS. Visualization of the immune landscape based on 65 cases of nHG-DCIS (*left*) and 52 cases of HG-DCIS (*right*). The connecting lines (*edges*) represent the correlation between the different cell populations. Edges with $r < 0.35$ and $r > -0.35$ were filtered out. Only positive correlations remained after filtering. The size of the nodes represents the mean percentage of the cell type in the cohort

DCIS tissue sections were stained for a panel of immune markers and analyzed with a multispectral imaging system. Multispectral imaging captures information from multiple wavelengths, not simply the red, green, and blue that our eyes see. This enables the disentangling of multiplex stains even when they are spatially overlapping, a task difficult for the human eye. Our automated image analyses correlated well with visual counts/scores by a pathologist. In particular, summing the automated counts of $CD4^+$, $CD8^+$, and $CD20^+$ lymphocytes correlated well with manual/visual scoring of tumor infiltrating lymphocytes, which can be a tedious process.

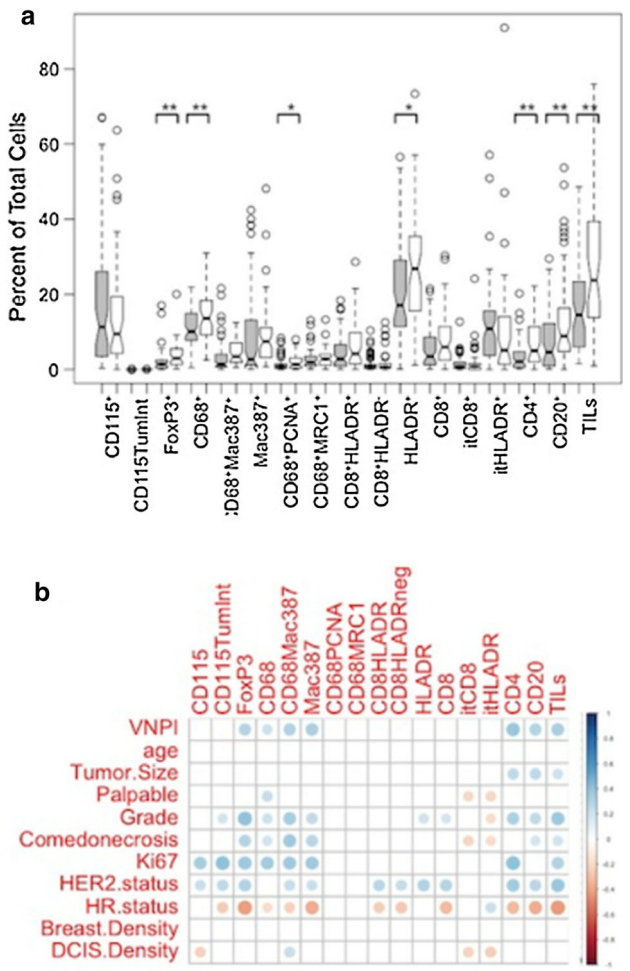

Fig. 5 Comparison of immune cell populations and clinicopathologic characteristics of DCIS. **a** Comparison of immune cell populations in high-grade versus non-high-grade DCIS. Gray boxes represent nHG-DCIS and white boxes represent HG-DCIS. Means were compared using Student's *t* test (*$p < 0.05$, **$p < 0.01$). **b** Correlations between immune markers and clinicopathologic characteristics. Dot color relates to the direction of the correlation (*red* negative correlation, *blue* positive correlation); color intensity and size of dots relates to the strength of the correlation. Only significant correlations are shown (Spearman's $p < 0.05$)

Using a panel of 117 DCIS cases, enriched for clinically high-grade DCIS (HG-DCIS; $n = 52$), we observed that percentages of $CD4^+$ T cells, $CD20^+$ B cells, and total TILs ($CD8^+$ T cells, $CD4^+$ T cells, plus $CD20^+$ B cells) were higher in HG-DCIS versus nHG-DCIS. This is consistent with previous studies that found increased inflammation associated with high nuclear grade in DCIS [30, 31]. We also observed higher levels of $CD68^+$ macrophages in HG-DCIS, consistent with our earlier study [13], as well as increased numbers of $CD68^+PCNA^+$ macrophages, which we have previously reported as being associated with poor outcomes in invasive breast cancer [19]. Finally, we found more $FoxP3^+$ cells (Treg cells) in HG-DCIS compared to nHG-DCIS.

Although we observed that various immune cell populations were correlated with high-risk features, none of these by themselves were correlated with recurrence events. This is consistent with a recently published study by Thompson et al. [36] who found, in a small cohort of 27 DCIS cases, trends for elevated numbers of $CD3^+$, $CD4^+$, $CD8^+$, $CD20^+$, and $FoxP3^+$ cells in ER-negative versus ER-positive cases, but none of these, individually, were associated with recurrences. To investigate whether combinations of immune cell populations and/or clinical risk factors were predictive of recurrence events, we performed a recursive partitioning and regression tree analysis. This analysis resulted in a classification tree comprised three cell populations: $CD8^+HLADR^+$ T cells, $CD8^+HLADR^-$ T cells, and $CD115^+$ macrophages. Interestingly, the $CD115^+$ cell population was more highly correlated with $CD8^+$ cell populations in HG-DCIS compared to nHG-DCIS cases (see Fig. 4). None of the clinical risk factors (grade, VNPI, tumor size, palpable, comedonecrosis, HR status, HER2 status, or DCIS density) were selected by the rpart algorithm.

Cases with low numbers of $CD8^+HLADR^+$ T cells had poor outcomes. Since HLA-DR is expressed on activated T cells, this would suggest that these cases may be lacking activated cytotoxic T cells targeting the DCIS or targeting invasive cancer cells that may arise from the DCIS. The other group with poor outcomes had not only $CD8^+HLADR^+$ T cells but also high numbers of $CD8^+HLADR^-$ T cells as well as high numbers of $CD115^+$ macrophages. The increased level of non-activated $CD8^+HLADR^-$ T cells would suggest a suppressive environment, possibly driven by the high numbers of $CD115^+$ macrophages. Indeed, we observed a significant positive correlation between $CD115^+$ macrophages and $CD8^+HLADR^-$ T cells (Spearman correlation; $p = 0.03$). These $CD115^+$ macrophages appear to be different than M2-type macrophages, as they are not highly correlated with the $CD68^+MRC1^+$ cell population. These results suggest that the adaptive immune response may play a role in preventing recurrence in DCIS. An independent validation study is warranted to confirm these results.

DCIS has always been characterized and treated based on pathologic criteria such as nuclear grade and size. More recently, a multigene expression assay, Oncotype DX DCIS, has been developed to predict recurrence risk for DCIS [37]. Interestingly, a study by Knopfelmacher et al. [38] found that a dense chronic inflammatory infiltrate around DCIS, defined as circumferential cuffing of the duct by lymphocytes or plasma cells at least three cell layers in thickness, was associated with a high Oncotype DX DCIS score. However, only 4 of the 45 cases studied had a high

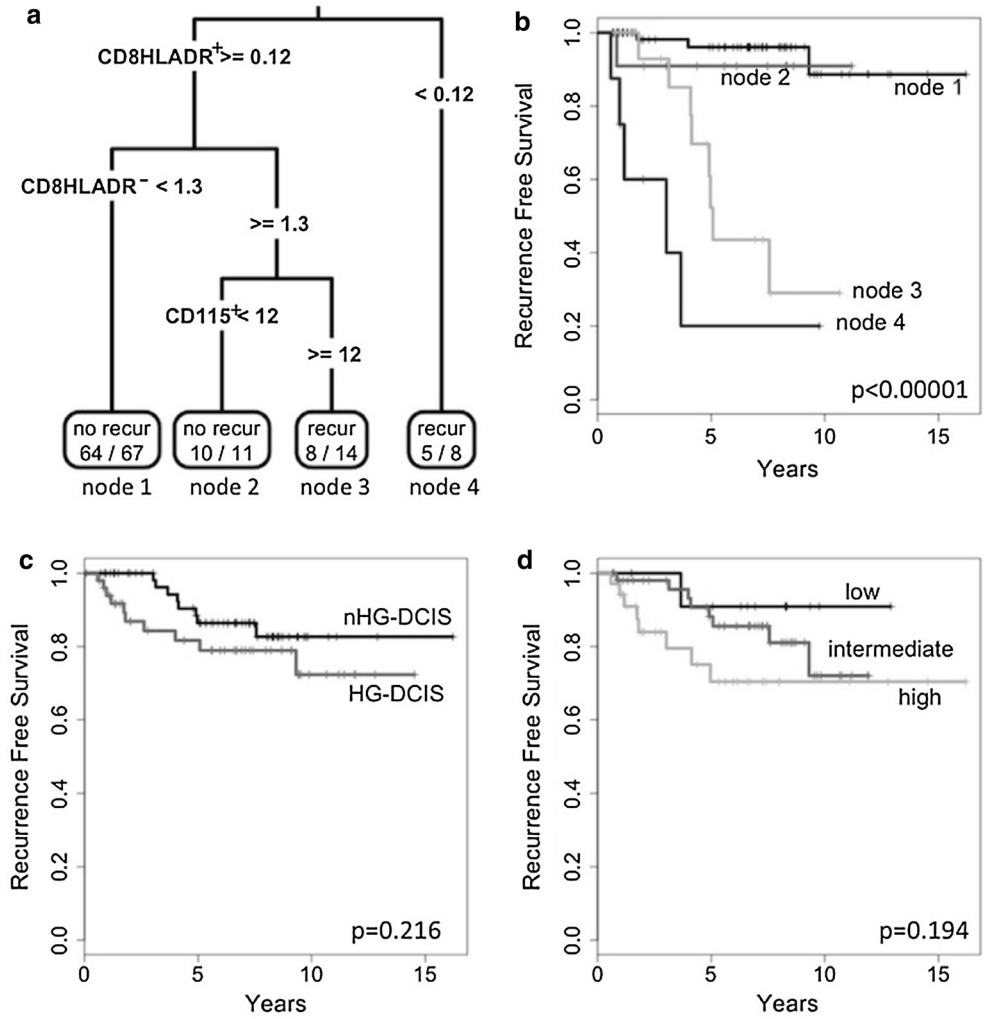

Fig. 6 Classification and Regression Tree analysis. **a** classification tree predicting recurrence events in DCIS based on immune cell infiltrates. Numbers in the end nodes represent the (number of correctly predicted cases)/(number of predicted cases) for that node. **b** Kaplan–Meier recurrence-free survival curves for DCIS cases based on the classification tree. **c** K–M curves for HG-DCIS versus nHG-DCIS. **d** K–M curves for DCIS cases separated by VNPI score

score and of these, only 2 showed dense periductal inflammation. As part of a subsequent validation study, we will obtain Oncotype DX DCIS scores on all cases to further define specific immune populations that may be associated with the Oncotype DX DCIS score.

The goal of the current study was to provide more insight into the biology of DCIS—at the level of the immune microenvironment—in order to catalyze new treatment approaches. These data support a way to identify the DCIS with highest risk for recurrence and suggest that immunotherapeutic strategies could be efficacious. The recent analysis done by Narod et al. shows that our current approach of treating DCIS with surgery followed by radiation therapy is not sufficient for the rare cases of DCIS that lead to breast cancer mortality [6]. The immune microenvironment is clearly different in high-risk lesions and offers an opportunity to find targeted ways to treat high-risk DCIS. We have initiated studies to determine whether we can activate the immune system and reverse these lesions to address the specific mortality risk these lesions pose.

Funding This work was supported by the Breast Cancer Research Foundation (Esserman), the National Institutes of Health, National Cancer Institute Grant P50 CA 58207 (Gray), and the Department of the Army, award: W81XWH-07-1-0663 and W81XWH-11-1-0549-BC100597P1 (Esserman, Gray, Baehner). The U.S. Army Medical Research Acquisition Activity, 820 Chandler Street, Fort Detrick, MD 21702-5014 is the awarding and administering acquisition office. The content of the information does not necessarily reflect the position or the policy of the Government, and no official endorsement should be inferred.

Compliance with ethical standards

Conflict of interest The authors declare that they have no conflict of interest.

Ethical approval All procedures performed in studies involving human participants were in accordance with the ethical standards of the institutional and/or national research committee and with the 1964 Helsinki declaration and its later amendments or comparable ethical standards.

Informed consent Informed consent was obtained from all individual participants included in the study.

References

1. Siziopikou KP (2013) Ductal carcinoma in situ of the breast: current concepts and future directions. Arch Pathol Lab Med 137(4):462–466. doi:10.5858/arpa.2012-0078-RA
2. Bianchi S, Vezzosi V (2008) Microinvasive carcinoma of the breast. Pathol Oncol Res 14(2):105–111. doi:10.1007/s12253-008-9054-8
3. Rosner D, Lane WW, Penetrante R (1991) Ductal carcinoma in situ with microinvasion. A curable entity using surgery alone without need for adjuvant therapy. Cancer 67(6):1498–1503
4. Solin LJ, Fowble BL, Yeh IT, Kowalyshyn MJ, Schultz DJ, Weiss MC, Goodman RL (1992) Microinvasive ductal carcinoma of the breast treated with breast-conserving surgery and definitive irradiation. Int J Radiat Oncol Biol Phys 23(5):961–968
5. Esserman L, Yau C (2015) Rethinking the standard for ductal carcinoma in situ treatment. JAMA Oncol 1(7):881–883. doi:10.1001/jamaoncol.2015.2607
6. Narod SA, Iqbal J, Giannakeas V, Sopik V, Sun P (2015) Breast cancer mortality after a diagnosis of ductal carcinoma in situ. JAMA Oncol 1(7):888–896. doi:10.1001/jamaoncol.2015.2510
7. Bijker N, Meijnen P, Peterse JL, Bogaerts J, Van Hoorebeeck I, Julien JP, Gennaro M, Rouanet P, Avril A, Fentiman IS, Bartelink H, Rutgers EJ (2006) Breast-conserving treatment with or without radiotherapy in ductal carcinoma-in situ: ten-year results of European Organisation for Research and Treatment of Cancer randomized phase III trial 10853—a study by the EORTC Breast Cancer Cooperative Group and EORTC Radiotherapy Group. J Clin Oncol 24(21):3381–3387. doi:10.1200/JCO.2006.06.1366
8. Bijker N, Peterse JL, Duchateau L, Julien JP, Fentiman IS, Duval C, Di Palma S, Simony-Lafontaine J, de Mascarel I, van de Vijver MJ (2001) Risk factors for recurrence and metastasis after breast-conserving therapy for ductal carcinoma-in situ: analysis of European Organization for Research and Treatment of Cancer Trial 10853. J Clin Oncol 19(8):2263–2271
9. Fisher B, Dignam J, Wolmark N, Mamounas E, Costantino J, Poller W, Fisher ER, Wickerham DL, Deutsch M, Margolese R, Dimitrov N, Kavanah M (1998) Lumpectomy and radiation therapy for the treatment of intraductal breast cancer: findings from National Surgical Adjuvant Breast and Bowel Project B-17. J Clin Oncol 16(2):441–452
10. Fisher B, Land S, Mamounas E, Dignam J, Fisher ER, Wolmark N (2001) Prevention of invasive breast cancer in women with ductal carcinoma in situ: an update of the National Surgical Adjuvant Breast and Bowel Project experience. Semin Oncol 28(4):400–418
11. Holmberg L, Garmo H, Granstrand B, Ringberg A, Arnesson LG, Sandelin K, Karlsson P, Anderson H, Emdin S (2008) Absolute risk reductions for local recurrence after postoperative radiotherapy after sector resection for ductal carcinoma in situ of the breast. J Clin Oncol 26(8):1247–1252. doi:10.1200/JCO.2007.12.7969
12. Houghton J, George WD, Cuzick J, Duggan C, Fentiman IS, Spittle M (2003) Radiotherapy and tamoxifen in women with completely excised ductal carcinoma in situ of the breast in the UK, Australia, and New Zealand: randomised controlled trial. Lancet 362(9378):95–102
13. Esserman LJ, Kumar AS, Herrera AF, Leung J, Au A, Chen YY, Moore DH, Chen DF, Hellawell J, Wolverton D, Hwang ES, Hylton NM (2006) Magnetic resonance imaging captures the biology of ductal carcinoma in situ. J Clin Oncol 24(28):4603–4610. doi:10.1200/JCO.2005.04.5518
14. Wai ES, Lesperance ML, Alexander CS, Truong PT, Moccia P, Culp M, Lindquist J, Olivotto IA (2011) Predictors of local recurrence in a population-based cohort of women with ductal carcinoma in situ treated with breast conserving surgery alone. Ann Surg Oncol 18(1):119–124. doi:10.1245/s10434-010-1214-x
15. Kurniawan ED, Rose A, Mou A, Buchanan M, Collins JP, Wong MH, Miller JA, Mann GB (2010) Risk factors for invasive breast cancer when core needle biopsy shows ductal carcinoma in situ. Arch Surg 145(11):1098–1104. doi:10.1001/archsurg.2010.243
16. Silverstein MJ (2003) The University of Southern California/Van Nuys prognostic index for ductal carcinoma in situ of the breast. Am J Surg 186(4):337–343
17. Silverstein MJ, Lagios MD (2015) Treatment selection for patients with ductal carcinoma in situ (DCIS) of the breast using the University of Southern California/Van Nuys (USC/VNPI) prognostic index. Breast J 21(2):127–132. doi:10.1111/tbj.12368
18. Adams S, Goldstein LJ, Sparano JA, Demaria S, Badve SS (2015) Tumor infiltrating lymphocytes (TILs) improve prognosis in patients with triple negative breast cancer (TNBC). Oncoimmunology 4(9):e985930. doi:10.4161/2162402X.2014.985930
19. Campbell MJ, Tonlaar NY, Garwood ER, Huo D, Moore DH, Khramtsov AI, Au A, Baehner F, Chen Y, Malaka DO, Lin A, Adeyanju OO, Li S, Gong C, McGrath M, Olopade OI, Esserman LJ (2011) Proliferating macrophages associated with high grade, hormone receptor negative breast cancer and poor clinical outcome. Breast Cancer Res Treat 128(3):703–711. doi:10.1007/s10549-010-1154-y
20. de la Cruz-Merino L, Barco-Sanchez A, Henao Carrasco F, Nogales Fernandez E, Vallejo Benitez A, Brugal Molina J, Martinez Peinado A, Grueso Lopez A, Ruiz Borrego M, Manuel Codes, de Villena M, Sanchez-Margalet V, Nieto-Garcia A, Alba Conejo E, Casares Lagar N, Ibanez Martinez J (2013) New insights into the role of the immune microenvironment in breast carcinoma. Clin Dev Immunol 2013:785317. doi:10.1155/2013/785317
21. Gu-Trantien C, Loi S, Garaud S, Equeter C, Libin M, de Wind A, Ravoet M, Le Buanec H, Sibille C, Manfouo-Foutsop G, Veys I, Haibe-Kains B, Singhal SK, Michiels S, Rothe F, Salgado R, Duvillier H, Ignatiadis M, Desmedt C, Bron D, Larsimont D, Piccart M, Sotiriou C, Willard-Gallo K (2013) CD4(+) follicular helper T cell infiltration predicts breast cancer survival. J Clin Investig 123(7):2873–2892. doi:10.1172/JCI67428
22. Ibrahim EM, Al-Foheidi ME, Al-Mansour MM, Kazkaz GA (2014) The prognostic value of tumor-infiltrating lymphocytes in triple-negative breast cancer: a meta-analysis. Breast Cancer Res Treat 148(3):467–476. doi:10.1007/s10549-014-3185-2
23. Jiang D, Gao Z, Cai Z, Wang M, He J (2015) Clinicopathological and prognostic significance of FOXP3$^+$ tumor infiltrating lymphocytes in patients with breast cancer: a meta-analysis. BMC Cancer 15(1):727. doi:10.1186/s12885-015-1742-7
24. Lee HJ, Park IA, Song IH, Shin SJ, Kim JY, Yu JH, Gong G (2015) Tertiary lymphoid structures: prognostic significance and relationship with tumour-infiltrating lymphocytes in triple-

negative breast cancer. J Clin Pathol 69(5):422–430. doi:10.1136/jclinpath-2015-203089
25. Matsumoto H, Koo SL, Dent R, Tan PH, Iqbal J (2015) Role of inflammatory infiltrates in triple negative breast cancer. J Clin Pathol 68(7):506–510. doi:10.1136/jclinpath-2015-202944
26. Miyashita M, Sasano H, Tamaki K, Hirakawa H, Takahashi Y, Nakagawa S, Watanabe G, Tada H, Suzuki A, Ohuchi N, Ishida T (2015) Prognostic significance of tumor-infiltrating $CD8^+$ and $FOXP3^+$ lymphocytes in residual tumors and alterations in these parameters after neoadjuvant chemotherapy in triple-negative breast cancer: a retrospective multicenter study. Breast Cancer Res 17(1):124. doi:10.1186/s13058-015-0632-x
27. Mukhtar RA, Nseyo O, Campbell MJ, Esserman LJ (2011) Tumor-associated macrophages in breast cancer as potential biomarkers for new treatments and diagnostics. Expert Rev Mol Diagn 11(1):91–100. doi:10.1586/erm.10.97
28. Obeid E, Nanda R, Fu YX, Olopade OI (2013) The role of tumor-associated macrophages in breast cancer progression (review). Int J Oncol 43(1):5–12. doi:10.3892/ijo.2013.1938
29. Watanabe MA, Oda JM, Amarante MK, Cesar Voltarelli J (2010) Regulatory T cells and breast cancer: implications for immunopathogenesis. Cancer Metastasis Rev 29(4):569–579. doi:10.1007/s10555-010-9247-y
30. Lee AH, Happerfield LC, Bobrow LG, Millis RR (1997) Angiogenesis and inflammation in ductal carcinoma in situ of the breast. J Pathol 181(2):200–206. doi:10.1002/(SICI)1096-9896(199702)181:2<200:AID-PATH726>3.0.CO;2-K
31. Ramachandra S, Machin L, Ashley S, Monaghan P, Gusterson BA (1990) Immunohistochemical distribution of c-erbB-2 in in situ breast carcinoma–a detailed morphological analysis. J Pathol 161(1):7–14. doi:10.1002/path.1711610104
32. Lal A, Chan L, Devries S, Chin K, Scott GK, Benz CC, Chen YY, Waldman FM, Hwang ES (2013) FOXP3-positive regulatory T lymphocytes and epithelial FOXP3 expression in synchronous normal, ductal carcinoma in situ, and invasive cancer of the breast. Breast Cancer Res Treat 139(2):381–390. doi:10.1007/s10549-013-2556-4
33. Sharma M, Beck AH, Webster JA, Espinosa I, Montgomery K, Varma S, van de Rijn M, Jensen KC, West RB (2010) Analysis of stromal signatures in the tumor microenvironment of ductal carcinoma in situ. Breast Cancer Res Treat 123(2):397–404. doi:10.1007/s10549-009-0654-0
34. Carpenter AE, Jones TR, Lamprecht MR, Clarke C, Kang IH, Friman O, Guertin DA, Chang JH, Lindquist RA, Moffat J, Golland P, Sabatini DM (2006) Cell Profiler: image analysis software for identifying and quantifying cell phenotypes. Genome Biol 7(10):R100. doi:10.1186/gb-2006-7-10-r100
35. Kamentsky L, Jones TR, Fraser A, Bray MA, Logan DJ, Madden KL, Ljosa V, Rueden C, Eliceiri KW, Carpenter AE (2011) Improved structure, function and compatibility for cell profiler: modular high-throughput image analysis software. Bioinformatics 27(8):1179–1180. doi:10.1093/bioinformatics/btr095
36. Thompson E, Taube JM, Elwood H, Sharma R, Meeker A, Warzecha HN, Argani P, Cimino-Mathews A, Emens LA (2016) The immune microenvironment of breast ductal carcinoma in situ. Mod Pathol 29(3):249–258. doi:10.1038/modpathol.2015.158
37. Solin LJ, Gray R, Baehner FL, Butler SM, Hughes LL, Yoshizawa C, Cherbavaz DB, Shak S, Page DL, Sledge GW Jr, Davidson NE, Ingle JN, Perez EA, Wood WC, Sparano JA, Badve S (2013) A multigene expression assay to predict local recurrence risk for ductal carcinoma in situ of the breast. J Natl Cancer Inst 105(10):701–710. doi:10.1093/jnci/djt067
38. Knopfelmacher A, Fox J, Lo Y, Shapiro N, Fineberg S (2015) Correlation of histopathologic features of ductal carcinoma in situ of the breast with the oncotype DX DCIS score. Mod Pathol 28(9):1167–1173. doi:10.1038/modpathol.2015.79